Effect of interface bonding on the transport properties in $CoFe_2/SrTiO_3/CoFe_2/NiFe$ magnetic tunnel junctions

R. Moubah, S. Colis,* F. Schleicher, N. Najjari, H. Majjad, G. Versini, S. Barre, C. Ulhaq-Bouillet, G. Schmerber, M. Bowen, and A. Dinia

Institut de Physique et Chimie des Matériaux de Strasbourg (IPCMS), UMR 7504 UDS-CNRS, UDS-ECPM, 23 Rue du Loess, BP 43, F-67034 Strasbourg Cedex 2, France

(Received 7 May 2010; revised manuscript received 18 June 2010; published 14 July 2010)

To test whether the interface between an Fe-alloy electrode and a $SrTiO_3$ (STO) tunnel barrier constitutes or not a good spin injector, we have studied the transport and magnetic properties of $CoFe_2$ (7.5 nm)/$SrTiO_3$ (3 nm)/$CoFe_2$ (1 nm)/NiFe (8 nm) stacks prepared by pulsed-laser deposition on STO(001) substrates and varied the STO barrier deposition temperature. While this parameter does not strongly influence the magnetic properties of the two electrodes, the resulting barrier height at the bottom $CoFe_2$/STO interface is lowered if the STO barrier is deposited at 300 °C rather than 80 °C and an already low-tunnel-magnetoresistance ratio is suppressed. We discuss our findings in terms of the oxide stability of the $CoFe_2$/STO interface.

DOI: 10.1103/PhysRevB.82.024415 PACS number(s): 75.76.+j, 85.75.−d

Magnetic tunnel junctions (MTJs) composed of two magnetic layers separated by an insulating barrier have been extensively studied due to their potential applications as magnetic memory-storage cells[1] or magnetic-field sensors.[2] In such systems, the electric resistance varies between two extreme values when the relative orientation of the magnetization of the two magnetic electrodes changes from parallel to antiparallel. The relative change in the resistance defines the tunnel magnetoresistance (TMR) ratio. According to the simple model of Jullière,[3] the use of materials with a high-spin polarization as magnetic electrodes in MTJs is supposed to lead to high-TMR values.[4] However, the spin polarization is very sensitive to the interface chemistry between the magnetic layers and the barrier, especially that in most cases the magnetic layers are metallic and the barrier is an oxide, and oxygen diffusion can occur.[5] Furthermore, it was demonstrated that the amplitude of the spin polarization and its sign depends not only on the nature of the magnetic materials but depends also on the nature of barrier.[6–10]

To increase the TMR ratio, one may study junctions with half-metallic electrodes, i.e., with a 100% spin polarization. Candidates include the $La_{0.7}Sr_{0.3}MnO_3$ (LSMO) manganite which, when associated with a STO tunnel barrier in LSMO/STO/LSMO junctions, may yield effective tunneling spin polarizations in excess of 99%.[11] Another candidate with a higher Curie temperature is Sr_2FeMoO_6 (SFMO),[12–15] which can also be matched with a STO barrier. In this vein, some of us investigated magnetotransport measurements on SFMO/STO/Co and SFMO/STO/$CoFe_2$ junctions. While the former yielded 50% TMR,[15] the latter yielded no TMR despite flat, sharp interfaces and an homogeneous barrier that was free of hot spots.[13] One possible explanation for this discrepancy is the spin polarization of the STO/$CoFe_2$ interface. Moreover, although this has thus far not been investigated, a $CoFe_2$ electrode could be also useful as hard magnetic electrode in hard-soft systems that can be easily pinned by a ferrimagnetic $CoFe_2O_4$ exchange-bias layer.[16,17] Such pinning layer could be therefore obtained by simply oxidizing the $CoFe_2$ metallic electrode.

The aim of our study is to better understand the spintronic properties of the $CoFe_2$/STO interface. We have therefore investigated the structural, magnetic, and transport properties of $CoFe_2/SrTiO_3/CoFe_2$/NiFe stacks prepared by pulsed-laser deposition. We find that varying the temperature at which the STO barrier was deposited can affect the TMR amplitude in lithographically processed junctions. We interpret our results in terms of the chemical stability of the $CoFe_2/SrTiO_3$ interface.

All samples were deposited by pulsed-laser deposition on STO(001) substrates using a KrF excimer laser ($\lambda = 248$ nm). The frequency and the energy density of the laser were kept at 10 Hz and 1.5 J/cm^2, respectively. The background pressure in the growth chamber was 3×10^{-8} mbar. Prior to deposition, the substrates were heated up to 500 °C during 15 min to desorb surface contaminants. All layers were deposited under vacuum (about 10^{-7} mbar) from commercially available targets. The lower $CoFe_2$ layer was grown at 300 °C. The STO barrier was deposited at either 300 °C (high-T STO) or 80 °C (low-T STO). After the STO barrier deposition, the top magnetic layer ($CoFe_2$/NiFe) was deposited at about 80 °C. A 2-nm-thick Ta layer was used to protect the sample against oxidation. The structural properties and the surface roughness of the different layers were analyzed by transmission electron microscopy (TEM) and reflection high-energy electron diffraction (RHEED). The TEM observations were carried out using a JEOL 2100 FCs microscope with a point to point resolution of 2.3 Å. The magnetic measurements were made at room temperature using an alternating gradient-field magnetometer. Junctions were then obtained by standard photolithography techniques.[18] The TMR ratio is defined as $\Delta R/R=(R_{AP}-R_P)/R_P$, where R_P and R_{AP} are the resistances of the junction in the parallel and antiparallel configurations of the magnetization vectors, respectively. A positive applied bias implies electron injection from the lower to the upper electrode.

We first discuss the growth mode and structure of our samples through *in situ* RHEED observations. Referring to Fig. 1(a), the RHEED pattern recorded along the [110]STO(001) (substrate) azimuth after the deposition of a 7.5-nm-thick $CoFe_2$ layer shows a continuous intensity along

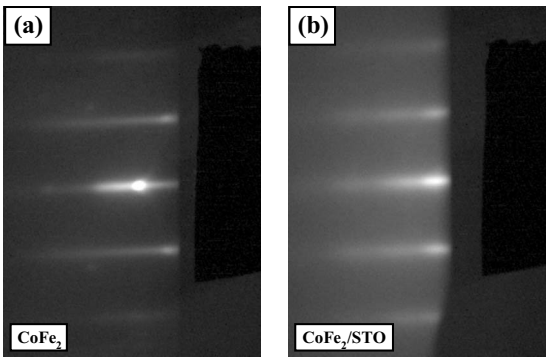

FIG. 1. *In situ* RHEED images recorded along the [100]STO(001) substrate azimuth obtained after the deposition of (a) a $CoFe_2$(7.5 nm) layer and (b) a $CoFe_2$(7.5 nm)/STO(3 nm) bilayer. The $CoFe_2$ layers were deposited at 300 °C while the STO barrier was deposited at 80 °C.

the streak length pointing out a two-dimensional (2D) growth mode. After the deposition at 80 °C of a 3-nm-thick STO barrier (low-*T* sample), the RHEED patterns recorded along the same azimuth also present a continuous intensity, which suggests a 2D growth mode and a well-defined crystalline structure [see Fig. 1(b)]. It is important to note that the intensity of the RHEED pattern of the STO barrier is smaller than that observed for $CoFe_2$. Such a reduction is probably due to the low-temperature deposition of the STO barrier (80 °C) with respect to that for the $CoFe_2$ bottom electrode (300 °C).

The cross-sectional image of a complete low-*T* STO stack [STO(001)/$CoFe_2$/STO/$CoFe_2$/NiFe/Ta] is shown in Fig. 2(a). The layers are continuous, with a fairly uniform thickness, and the interfaces are sharp and free of oscillations. The upper and lower junction interfaces appear to be of similar quality, in agreement with the RHEED results. We infer a $CoFe_2$ thickness of 7.6 ± 0.2 nm; 3.1 ± 0.2 nm for the STO barrier; 8.3 ± 0.2 nm for the $CoFe_2$/NiFe electrode, and 2 ± 0.2 nm for the Ta layer. The high-resolution TEM image [Fig. 2(b)] shows that the $CoFe_2$ bottom layer and the STO barrier are monocrystalline, as already pointed out by the RHEED observations. The $CoFe_2$(100) planes are visible and perpendicular to the film surface. We can also see that the (110) planes of the STO barrier are oriented at 45° with respect to the film surface. The epitaxy relation between the substrate, bottom magnetic layer and barrier is $[100]STO_{substrate}(001) \| [110]CoFe_2(001) \| [100]STO_{barrier}(001)$. The $CoFe_2$ lattice is therefore rotated in plane by 45° with respect to that of STO. It is interesting to point out that, although the barrier is deposited at low temperature, its structure is monocrystalline as we have reported previously.[12–14] Finally, the $CoFe_2$/NiFe top electrode exhibits a polycrystalline structure: atomic planes are visible but their orientation is not well defined. This likely underscores the low-deposition temperature of the top electrode. We note that the upper STO/$CoFe_2$ interface in SFMO/STO/$CoFe_2$ stacks with the STO and $CoFe_2$ deposited in the same conditions as in our samples was already investigated by means of electron energy loss spectroscopy and that no atomic diffusion could be detected.[14]

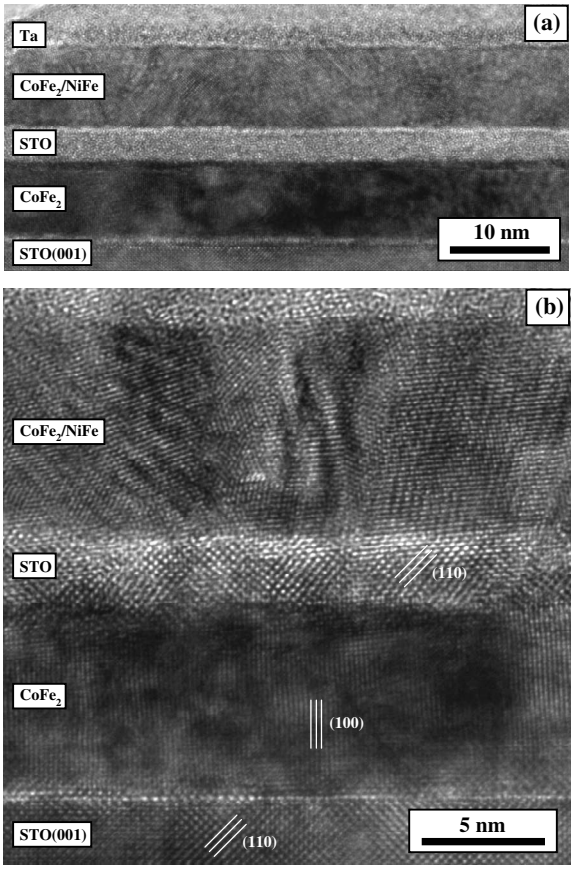

FIG. 2. (a) Low magnification and (b) high-resolution cross-sectional TEM images of a $CoFe_2$ (7.5 nm)/$SrTiO_3$ (3 nm)/$CoFe_2$ (1 nm)/NiFe (8 nm)/Ta (2 nm) low-*T* STO stack.

Figure 3 shows the magnetization curve of low-*T* STO and high-*T* STO $CoFe_2$/STO/$CoFe_2$/NiFe stacks. The magnetic field was applied in the film plane along the [100]STO(001) substrate direction. In both cases, the major loop displays two sharp transitions that correspond to the reversal of the top and bottom electrode magnetizations, respectively. The coercive fields of the bottom and top elec-

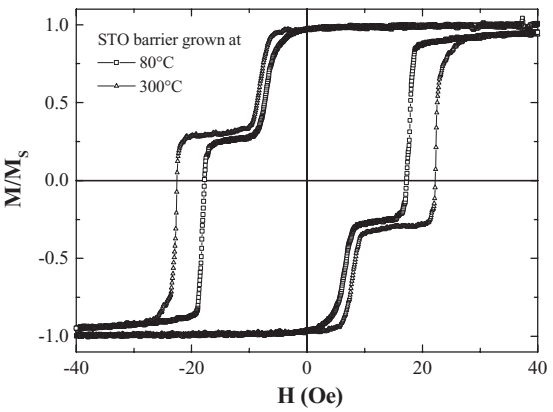

FIG. 3. Room-temperature magnetization curves of $CoFe_2$ (7.5 nm)/$SrTiO_3$ (3 nm)/$CoFe_2$ (1 nm)/NiFe (8 nm)/Ta (2 nm) stacks with a STO barrier grown at 80 and 300 °C. The magnetic field was applied along the [100]STO(001) direction.

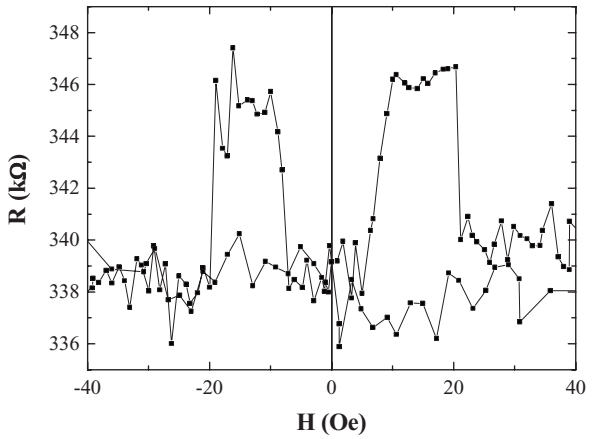

FIG. 4. Room-temperature *R-H* curve of a 20 μm diameter $CoFe_2$ (7.5 nm)/$SrTiO_3$ (3 nm)/$CoFe_2$ (1 nm)/NiFe (8 nm)/Ta (2 nm) MTJ processed from a low-*T* STO stack.

trodes of the low-*T* STO stack are $H_{C1} \sim 7$ Oe and $H_{C2} \sim 18$ Oe, respectively. These values increase slightly for the high-*T* STO sample to about 8 and 22 Oe. This indicates a possible oxidation of $CoFe_2$ at the $CoFe_2$/STO interfaces. The deposition at low temperature, rather than at high temperature, of the STO barrier therefore seems to result in sharper interfaces. Additional measurements recorded in a field applied along the [110]STO(001) direction (data not shown) reveal a slight anisotropy for the bottom $CoFe_2$ layer while no anisotropy could be detected in the top $CoFe_2$/NiFe electrode. This is consistent with the TEM observation of a monocrystalline and polycrystalline structure for the bottom and top electrodes, respectively.

Figure 4 shows the room-temperature magnetic-field dependence of the resistance of a circular 20 μm diameter $CoFe_2$(7.5 nm)/$SrTiO_3$ (3 nm)/$CoFe_2$ (1 nm)/NiFe (8 nm)/Ta (2 nm) junction processed from a low-*T* STO stack. The resistance increases sharply at about 7 Oe and decreases at about 20 Oe, in good agreement with the switching fields evidenced in the magnetic-hysteresis curve (see Fig. 3). Surprisingly, the TMR ratio is about 3%, which is much smaller than that expected by simply considering the spin polarization at the Fermi level E_F of the similar alloy CoFe of 50%.[5] No TMR was measured on junctions processed from a high-*T* STO stack (data not shown).

One possible explanation lies with the symmetry of the electron wave functions that may favorably transmit through the STO barrier. Indeed, while a MgO barrier favors Δ_1 transmission, a STO barrier favors $\Delta_{2',5}$ transmission.[19] bcc-ordered Fe and Co-Fe alloys exhibit a band with Δ_1 symmetry that crosses E_F only for majority spins. In contrast, such a spin polarization of $\Delta_{2',5}$ symmetries occurs only for a sufficiently Co-rich Co-Fe alloy.[20] It is possible that the band structure of our Fe-rich Co-Fe alloy does not exhibit a spin polarization at E_F of the $\Delta_{2',5}$ symmetries.

An additional factor that can limit the TMR in our samples is the chemical structure of the STO barrier at the interface. Indeed, in our samples we have shown that the barrier is monocrystalline with the STO(001) planes parallel to the film surface. This means that, along the [001]STO direction, the barrier is constituted of alternating SrO and TiO_2 planes that may form the interface with the $CoFe_2$ layer. Yet, it was recently shown that a STO/Co interface may exhibit positive (negative) spin polarization if the STO is SrO (TiO_2) terminated.[21] Since the last atomic plane of the STO barrier cannot be easily controlled, the low sign of TMR could thus reflect a mixing of SrO and TiO_2 terminations at one or both of the junction interfaces, leading to low-effective values of spin polarization of the interfaces and thus to a low TMR value. This issue of interface termination is absent in the case of MgO barriers since only one metallic species is present in that oxide.

TABLE I. Enthalpy of formation of oxides commonly used in MTJ systems. The values are extracted from Ref. 28.

Oxide	Enthalpy of formation (kcal/mol)
Al_2O_3	−404
MgO	−144
SrO	−142
TiO_2	−228
CoO	−57
FeO	−65

A third possible explanation pertains to the oxidation state of $CoFe_2$ at the junction interface. Indeed, we note that the large spin polarization of CoFe was obtained when paired to a MgO barrier.[22,23] On the other hand, pairing an electrode containing Fe to a STO barrier has generally led to low-TMR ratios.[24,25] We note, in particular, a similarly low TMR of 2% at room temperature in CoFeB/STO/CoFeB MTJs.[26] In general terms, an electrode containing Fe may, when paired with an oxide barrier, lead to an interface with reasonable spintronic properties if the oxide has a large enthalpy of oxide formation such as MgO (Refs. 22 and 23) or Al_2O_3 (Refs. 27 and 28) (see Table I). We note that both MgO as well as SrO and TiO_2 in STO, have an enthalpy of oxide formation of the same order of magnitude. We also note that Fe-O bonds may form more easily than Co-O (see Table I). This hypothesis is supported by the absence of TMR in MTJs processed from high-*T* STO stacks, for which the higher energy of the atoms during the growth process of STO may favor the formation of Fe oxide at the interface. This could in turn explain the somewhat larger coercive fields observed in the high-*T* STO stack (Fig. 3).

To test our hypothesis of interfacial Fe oxide formation, we now examine the barrier heights at both the top and bottom interfaces. We present in Fig. 5 the *I-V* curves obtained on MTJs processed from both low-*T* STO and high-*T* STO stacks. The barrier thickness and height can be obtained by fitting the curves within the Brinkman model.[29] The barrier thickness is equal to 2.7 nm for both samples and close to that observed by TEM (3.1 nm). A fit of the barrier height at the top interface yields a value of 0.61 eV for both low-*T* STO and high-*T* STO stacks. This identical value is expected since for both stack types, the top $CoFe_2$ electrode is deposited at about 80 °C. On the other hand, the barrier heights at

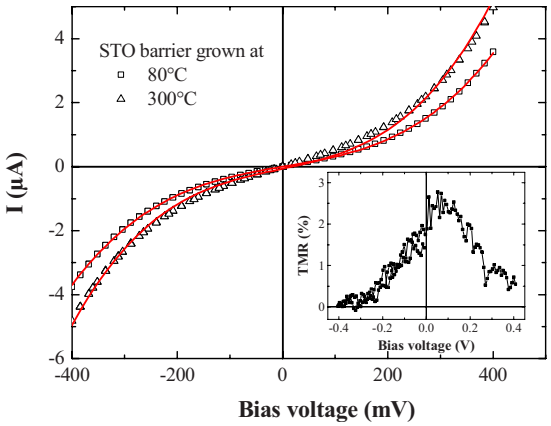

FIG. 5. (Color online) Room-temperature *I-V* curve on MTJs processed from low-*T* STO and high-*T* STO stacks. The continuous lines stem for the Brinkman-fit curves. Inset: typical TMR bias dependence of MTJs from a low-*T* STO stack.

the lower interface are only of 0.51 and 0.38 eV for low-*T* STO and high-*T* STO MTJs, respectively. These reduced values underscore the impact of oxidation considerations at the lower interface, which are enhanced when the STO barrier is deposited at high temperature. In support of this argument, the bias dependence of TMR found on low-*T* STO MTJs is asymmetric (see inset of Fig. 5) and decreases more slowly at a positive sign of applied bias that corresponds to electron injection at E_F from the lower interface to states at $E=E_F+eV$ of the upper one. This spin-polarized response thus also supports our conclusion that the top interface is spintronically more performing than the lower one due to a likely oxidation issue at the lower interface.

In summary, we have studied the consequence of different deposition temperatures of the STO barrier on the structural, magnetic, and magnetotransport properties of $CoFe_2/STO/CoFe_2/NiFe$ stacks. The magnetization curves of all samples show a two-step reversal of the magnetization related to the switching of the $CoFe_2$ and $CoFe_2/NiFe$ magnetizations. However, increasing the deposition temperature of the STO barrier leads to a vanishing of the otherwise small TMR ratio. We discuss this effect and the low TMR ratio, in terms of electronic symmetry, a mixing of the interface termination and, more likely, interfacial oxidation considerations. Our experiments on STO barriers underscore the need to pair transition-metal oxide barriers with electrodes with a low enthalpy of oxidation.

We acknowledge ANR Contract SpinMarvel (Contract No. ANR-09-JCJC-0137) for financial support.

*colis@ipcms.u-strasbg.fr

[1] S. A. Wolf, D. D. Awschalom, R. A. Buhrman, J. M. Daughton, S. von Molnar, M. L. Roukes, A. Y. Chtchelkanova, and D. M. Treger, Science **294**, 1488 (2001).
[2] M. Pannetier, C. Fermon, G. Le Goff, J. Simola, and E. Kerr, Science **304**, 1648 (2004).
[3] M. Jullière, Phys. Lett. **54A**, 225 (1975).
[4] S. Yuasa, T. Nagahama, A. Fukushima, Y. Suzuki, and K. Ando, Nature Mater. **3**, 868 (2004).
[5] S. Colis, G. Gieres, L. Bär, and J. Wecker, Appl. Phys. Lett. **83**, 948 (2003).
[6] J. M. De Teresa, A. Barthélémy, A. Fert, J. P. Contour, F. Montaigne, and P. Seneor, Science **286**, 507 (1999).
[7] T. Dimopoulos, G. Gieres, S. Colis, J. Wecker, Y. Luo, and K. Samwer, Appl. Phys. Lett. **83**, 3338 (2003).
[8] S. Colis, G. Gieres, T. Dimopoulos, L. Bär, and J. Wecker, IEEE Trans. Magn. **40**, 2287 (2004).
[9] M. Guth, A. Dinia, G. Schmerber, and H. A. M. Van den Berg, Appl. Phys. Lett. **78**, 3487 (2001).
[10] T. Dimopoulos, G. Gieres, S. Colis, R. Lopez, M. Vieth, J. Wecker, Y. Luo, and K. Samwer, IEEE Trans. Magn. **40**, 2296 (2004).
[11] M. Bowen, J. L. Maurice, A. Barthélémy, M. Bibes, D. Imhoff, V. Bellini, R. Bertacco, D. Wortmann, P. Seneor, E. Jacquet, A. Vaures, J. Humbert, J. P. Contour, C. Colliex, S. Blugel, and P. H. Dederichs, J. Phys.: Condens. Matter **19**, 315208 (2007).
[12] T. Fix, A. Barla, C. Ulhaq-Bouillet, S. Colis, J. P. Kappler, and A. Dinia, Chem. Phys. Lett. **434**, 276 (2007).
[13] T. Fix, V. Da Costa, C. Ulhaq-Bouillet, S. Colis, A. Dinia, K. Bouzehouane, and A. Barthélémy, Appl. Phys. Lett. **91**, 083104 (2007).
[14] T. Fix, C. Ulhaq-Bouillet, S. Colis, A. Dinia, G. Bertoni, J. Verbeeck, and G. Van Tendeloo, Appl. Phys. Lett. **91**, 023106 (2007).
[15] M. Bibes, K. Bouzehouane, A. Barthélémy, M. Besse, S. Fusil, M. Bowen, P. Seneor, J. Carrey, V. Cros, A. Vaures, J. P. Contour, and A. Fert, Appl. Phys. Lett. **83**, 2629 (2003).
[16] T. Fix, S. Colis, K. Sauvet, J. L. Loison, G. Versini, G. Pourroy, and A. Dinia, J. Appl. Phys. **99**, 043907 (2006).
[17] S. Maat and B. A. Gurney, J. Appl. Phys. **93**, 7229 (2003).
[18] D. Halley, H. Majjad, M. Bowen, N. Najjari, Y. Henry, C. Ulhaq-Bouillet, W. Weber, G. Bertoni, J. Verbeeck, and G. Van Tendeloo, Appl. Phys. Lett. **92**, 212115 (2008).
[19] M. Bowen, A. Barthélémy, V. Bellini, M. Bibes, P. Seneor, E. Jacquet, J. P. Contour, and P. H. Dederichs, Phys. Rev. B **73**, 140408(R) (2006).
[20] S. Yuasa, A. Fukushima, H. Kubota, Y. Suzuki, and K. Ando, Appl. Phys. Lett. **89**, 042505 (2006).
[21] I. J. Vera Marún, F. M. Postma, J. C. Lodder, and R. Jansen, Phys. Rev. B **76**, 064426 (2007).
[22] Y. M. Lee, J. Hayakawa, S. Ikeda, F. Matsukura, and H. Ohno, Appl. Phys. Lett. **90**, 212507 (2007).
[23] D. D. Djayaprawira, K. Tsunekawa, M. Nagai, H. Maehara, S. Yamagata, N. Watanabe, S. Yuasa, Y. Suzuki, and K. Ando, Appl. Phys. Lett. **86**, 092502 (2005).
[24] J. Z. Sun, K. P. Roche, and S. S. P. Parkin, Phys. Rev. B **61**, 11244 (2000).
[25] J. Hayakawa, K. Ito, S. Kokado, M. Ichimura, A. Sakuma, M. Sugiyama, H. Asano, and M. Matsui, J. Appl. Phys. **91**, 8792 (2002).

[26] K. Oguz and J. M. D. Coey, J. Magn. Magn. Mater. **321**, 1009 (2009).
[27] S. Yuasa, T. Sato, E. Tamura, Y. Suzuki, H. Yamamoi, K. Ando, and T. Katayama, Europhys. Lett. **52**, 344 (2000).
[28] *CRC Handbook of Chemistry and Physics*, R. C. Weast and M. J. Astle, 59th ed. (CRC Press, Boca Raton, 1978).
[29] W. F. Brinkman, R. C. Dynes, and J. M. Rowell, J. Appl. Phys. **41**, 1915 (1970).